Chapter 5
Current Imaging Approaches and Challenges in the Assessment of Carotid Artery Disease

Krishnan Ravindran, Waleed Brinijiki, J. Kevin DeMarco, and John Huston III

MR Angiography in Vessel Wall Imaging of the Internal Carotid Artery

Introduction

MRI has historically been the most well-established imaging modality for carotid plaque characterization due to its high signal-to-noise ratio and its establishment as the gold standard for carotid plaque imaging when compared to histological gold standards. Both intraplaque hemorrhage and lipid-rich necrotic core can be detected with high sensitivity and specificity on MRI and, importantly, good inter-observer agreement. Its noninvasive nature, lack of radiation exposure, and high soft tissue contrast enable detailed visualization of plaque morphology. There are a wide variety of pulse sequences available for plaque characterization with MRI. Fast spin echo (FSE) is the most commonly used technique as it allows for T1-, T2-, and proton density (PD)-weighted imaging. Gradient echo imaging with or without inversion recovery preparatory pulses is another technique for rapid imaging acquisition which has high reliability to detect plaque hemorrhage and lipid-rich necrotic core on T1-weighted images. This method uses FSE sequences with double inversion recovery preparatory pulses, thus resulting in a high amount of contrast between the dark vessel lumen and the vessel wall.

K. Ravindran · W. Brinijiki (✉) · J. Huston III
Department of Radiology, Mayo Clinic, Rochester, MN, USA
e-mail: Brinjikji.Waleed@mayo.edu; jhuston@mayo.edu

J. K. DeMarco (✉)
Department of Radiology, Walter Reed National Military Medical Center, Bethesda, MD, USA

Department of Radiology, Uniformed Services University of the Health Sciences, Bethesda, MD, USA

C. Yuan et al. (eds.), *Vessel Based Imaging Techniques*,
https://doi.org/10.1007/978-3-030-25249-6_5

Fat suppression is absolutely essential for characterization of plaque morphology. This method is needed to suppress signal of subcutaneous fat resulting in a high degree of contrast between plaque components, the carotid wall and surrounding tissues. Administration of gadolinium-based contrast aids delineation of plaque morphology and differentiation of core from fibrous cap on T1 sequences [1]. Contrast enhancement is believed to be associated with plaque inflammation and neovascularization [2]. Neovascularity is seen in nearly 100% of contrast-enhancing areas and the histological presence of macrophage infiltration in nearly 90% of post-contrast-enhancing regions [3]. MRI findings correlate strongly with histopathological findings of plaque morphology and have high specificity/sensitivity and inter-observer agreement [4]. Antibody-coated superparamagnetic iron oxide particles have also been used as an alternative potential contrast agent and shown to reflect histological plaque inflammation and endothelial activation [5].

Intraplaque Hemorrhage

MRI is excellent at detecting intraplaque hemorrhage [6, 7]. Intraplaque hemorrhage is often located diffusely in the plaque and colocalizes with lipid-rich necrotic core. Intraplaque hemorrhage is optimally evaluated on T1-weighted and fat-/flow-suppressed sequences as hemoglobin products induce T1 shortening [8, 9]. Black-blood sequences using T1-weighted imaging with fat saturation or MPRAGE-type sequences demonstrate plaque hemorrhage as T1 hyperintense with signal intensities at least 50% higher than the adjacent sternocleidomastoid muscle. These sequences suppress flow artifact near the carotid bifurcation, though increasing the time for examination. Plaque hemorrhage can easily be identified using both surface coil imaging techniques and large field-of-view MPRAGE imaging using standard head and neck coils. The sensitivity of specificity of plaque hemorrhage identification using surface coils is about 98% compared to histological gold standard, while the sensitivity of plaque hemorrhage identification of surface coils compared to MPRAGE imaging is well over 90%. Figure 5.1 shows an example of intraplaque hemorrhage.

Plaque hemorrhage signal intensities can change over time. Fresh plaque hemorrhage is hyperintense on T1-weighted images and hypointense/isointense on T2-weighted images and PD-weighted images. Both hemorrhage and lipid-rich core may exhibit high T1 signal. These can be distinguished on T1-weighted time-of-flight (TOF) sequences, with hemorrhage typically appearing hyperintensing on both T1 and TOF. Proton density-weighted sequences are also used, though plaque hemorrhage appearance on this sequence is more variable. In a study of 26 patients undergoing TOF and T1- and T2-weighted imaging prior to endarterectomy, MRI was able to differentiate intraplaque hemorrhage from juxtaluminal hemorrhage with near 100% accuracy [10]. Recent plaque hemorrhage is hyperintense on all contrast weightings. In a study of 42 plaques with recent intraplaque hemorrhage, Yim and colleagues demonstrated the presence of a peripheral rim of high signal intensity (“halo sign”) around the carotid on maximum intensity project images of

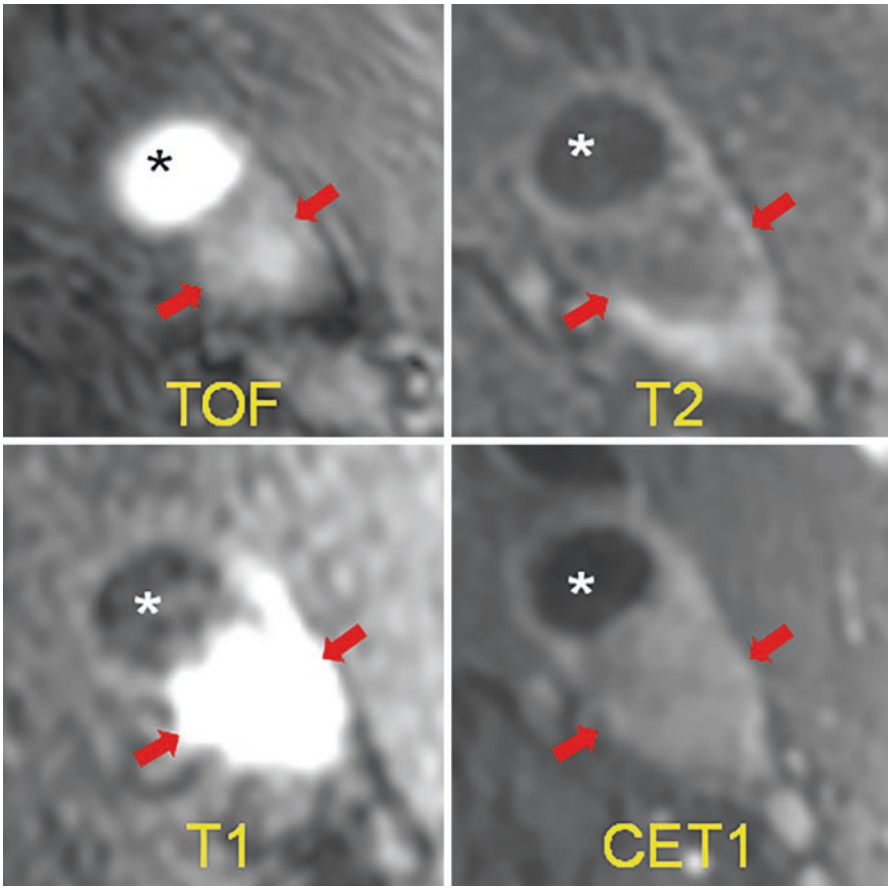

Fig. 5.1 Example of intraplaque hemorrhage on surface coil MRI at 3T. Time of flight (TOF) shows a widely patent lumen (∗) with a large plaque associated with positive remodeling, which is T1 hyperintense (arrows). On T2, the lumen (∗) is widely patent, and there is T2 hypointensity within the plaque. On MPRAGE, we see the patent lumen (∗) with marked T1 hyperintensity in the carotid plaque consistent with hemorrhage. On the contrast-enhanced T1 weighted image (CET1), the plaque is again seen with minimal internal enhancement but robust enhancement of the adventitia. (*J* jugular vein)

TOF MRI [11]. The negative predictive value of this halo sign on TOF MR angiography was 95%. The T1 hyperintensity of plaque hemorrhage can last for months to years following the initial event. However, older plaque hemorrhage has been reported to appear hypointense on all contrast weightings [12].

In asymptomatic individuals with 50–70% carotid stenosis, the presence of intraplaque hemorrhage on MRI was associated with a markedly increased risk of cerebrovascular events [13] (hazard ratio 3.59, 95% confidence interval 2.48–4.71, $p < 0.001$). In a further meta-analysis of 689 patients undergoing carotid MRI, the event rate for cerebrovascular events was 17.8% per year, compared to 2.4% in patients without MRI-visible intraplaque hemorrhage [14].

Lipid-Rich Necrotic Core

Lipid-rich necrotic core is best identified on MRI black-blood vessel wall imaging. Lipid-rich necrotic core is identified using a combination of T1 fat-saturated black-blood imaging with and without contrast. Lipid-rich necrotic core consists of a hypointense plaque on T1 fat-saturated imaging with an associated internal hypointense/non-enhancing region. Unlike plaque hemorrhage, necrotic core typically appears hyperintense on T1-weighted sequences but isointense on TOF images. The lack of internal enhancement indicates necrotic lipid which is not vascularized. The sensitivity and specificity of surface coil imaging at 3T in identification of LRNC are also over 95% when compared to histological controls. When compared to a surface coil exam, imaging of carotid plaques with standard head and neck coils has a sensitivity and specificity of about 85–90% for identification of lipid-rich necrotic core. Unlike ultrasound, MRI is able to distinguish lipid-rich core from hemorrhage and calcification with high sensitivity and specificity. Single-sequence T1-weighted turbo field echo (TFE) MRI has been shown to be as good, if not superior, to multi-sequence MRI in quantifying lipid-rich necrotic core with inter-reader reproducibility above 0.90 [15]. Contrast-enhanced MRI importantly allows discrimination of fibrous cap from necrotic core; given the avascular nature of the core, it displays minimal contrast enhancement, while the surrounding fibrous tissue has been shown to display strong enhancement [16]. In this study, the authors further identified a subset of lesions that hyper-enhanced with contrast administration, which was histologically corroborated with the presence of plaque neovascularization. Use of high-resolution contrast-enhanced MRI furthermore enables in vivo quantification of fibrous cap length and area [17]. T2-weighted sequences have been suggested to overestimate lipid core volume [18]. Moreover, the presence of hemorrhage within the lipid-rich necrotic core may result in T2 hyperintensity and make delineation of fibrous cup and necrotic core difficult. On high-resolution contrast-enhanced MRI, hemorrhage showed minimal enhancement making lipid-rich necrotic core delineation easier. Figure 5.2 shows an example of lipid-rich necrotic core.

MRI Plaque Features and Prognosis

Plaque enhancement with gadolinium visualized using 3T MRI is strongly associated with plaque vulnerability and cerebrovascular ischemic events, independent of wall thickness and degree of stenosis [19]. Indeed, MRI biomarkers of carotid plaque show stronger association with the presence of clinical symptoms than degree of luminal stenosis [1]. In a meta-analysis of nine studies (779 patients) assessing plaque characteristics and clinical prognosis, incidence of future transient ischemic attack or stroke was more than three times higher with the presence of either intraplaque hemorrhage or lipid-rich necrotic core [20]. Taken together, these results suggest characterization of plaque morphology and composition using MRI

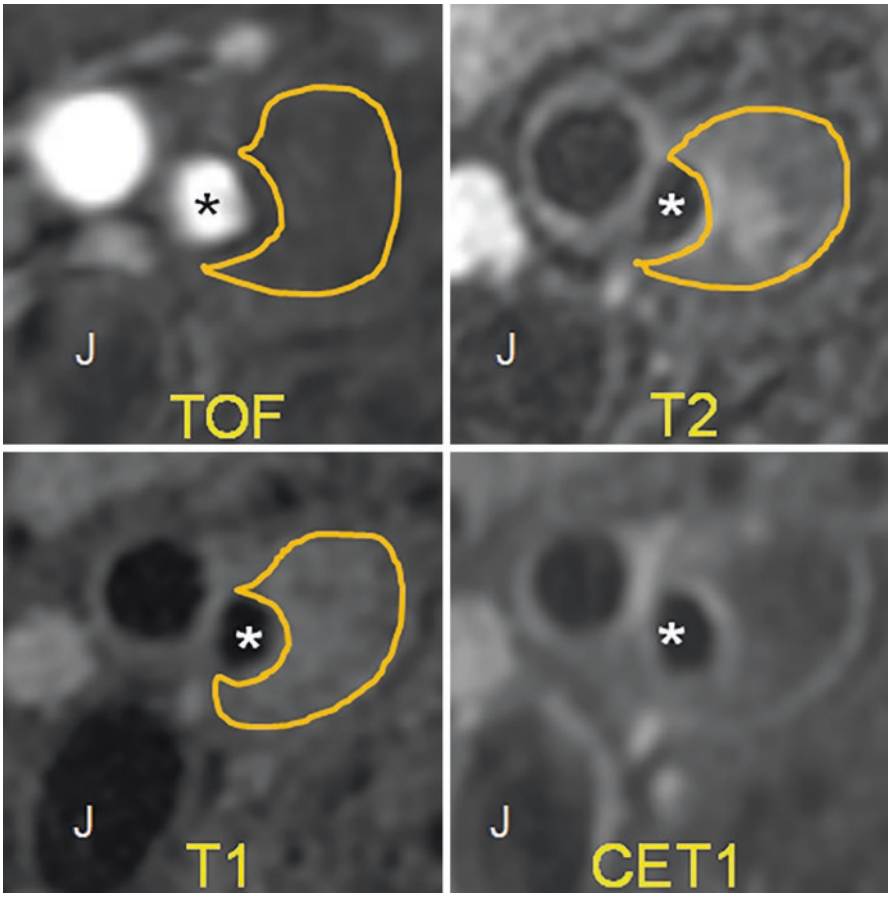

Fig. 5.2 Example of lipid-rich necrotic core. TOF shows a patent carotid artery lumen (∗). There is a large plaque with positive remodeling, which does not have any internal hyperintensity. On T2, there is some internal hyperintensity, but for the most part, the plaque is hypointense. On the T1 fat-saturated image, we see internal hypointensity. On the contrast-enhanced T1 image (CET1), there is peripheral enhancement of the plaque and no internal enhancement. This is characteristic of lipid-rich necrotic core

techniques may indeed provide greater information for risk stratification than quantitative stenosis measurement.

MRI Summary

MRI is highly specific and sensitive for plaque morphology, and features of plaque vulnerability on MRI correlate well with risk of future cerebrovascular events across several studies. Literature assessing the role of multiple contrast-weighted MRI in

evaluating carotid plaque has substantially increased. Expense and availability remain limiters in certain populations. Importantly, MRI findings also corroborate very strongly with histological findings, suggesting MRI with multiple contrast weightings may be an important tool for selecting candidate patients for intervention. Notably, plaque morphology findings may not be fully concordant with MR angiographic stenosis, particularly in predicting risk of future transient ischemic attacks or stroke.

CT Angiography in Vessel Wall Imaging of the Carotid Artery

Introduction

Multi-detector row CT angiography (CTA) is an easy and rapid imaging modality to detect extracranial carotid stenosis. The role of CTA to evaluate carotid vessel wall abnormality is less clear. Compared with the robust, extensive literature describing the MR imaging characteristics of vulnerable carotid plaque features, there is less literature and less consensus on the vulnerable plaque detection using CTA. Carotid CT vessel wall imaging (VWI) to detect various components in the soft plaque has been limited by overlapping Hounsfield units (HU) and blurring/blooming effect of extensive plaque calcifications (CA). Nevertheless, exciting new research indicates that vulnerable plaque features can be detected using CTA. We will review the CTA appearance of lipid-rich necrotic core (LRNC) which is associated with the American Heart Association lesion type IV/V (AHA-LT4/5). Next, we look at multiple different techniques that have been proposed to detect intraplaque hemorrhage (IPH) seen in American Heart Association lesion type VI (AHA-LT6) plaques. Lastly, we will look at research evaluating the ability of CTA to measure fibrous cap and/or identify fissured fibrous cap.

Lipid-Rich Necrotic Core

Carotid CTA can differentiate between soft tissue and calcified plaque. The use of simple Hounsfield units (HU) to detect LRNC on carotid CTA has led to inconsistent results. Some of the initial poor correlation of CTA-detected LRNC and histology was probably related to partial volume artifacts due to the use of single-slice CTA with thick axial images. Even with the use of more modern multi-detector CT (MDCT) scanners with thinner axial slices, partial volume effects still limit the detection of smaller LRNC regions. Also, extensive carotid plaque CA can lead to blurring/blooming which limits detection of adjacent soft tissue plaque including LRNC. Recent post-processing algorithms can mitigate both the blurring and partial volume effects to more accurately detect and quantify carotid plaque LRNC.

Initial studies comparing the detection of LRNC on CTA with histological evaluation of carotid endarterectomy specimens (CEA) utilized a single-slice spiral CT

scanner with axial images reconstructed every 1.5 mm. In a review of 55 patients undergoing CEA who underwent single-slice spiral CTA preoperatively, there was a statistically significant decrease in HU density measurements with increasing plaque lipid but with high standard deviation of these values [21]. The authors concluded that analysis of plaque attenuation does not give useful information concerning plaque composition.

In a subsequent study in 15 symptomatic patients with severe carotid stenosis who underwent a carotid CTA just prior to CEA using a 16-slice MDCT scanner with axial images reconstructed at 0.6 mm intervals, the measured attenuation value of LRNC was 25 HU ± 19 HU with a cutoff of 60 HU to differentiate between LRNC and fibrous tissue [22]. However, the regression plots showed good correlation of LRNC size measured on CTA compared with CEA specimen histology ($R^2 = 0.77$) only in mildly calcified carotid plaques (0–10%). The authors hypothesized that the lack of correlation between LRNC HU measurements in more densely CA plaque and histology could be explained by the blooming effect of CA on CTA.

Wintermark et al. described their comparison of eight patients with recent TIA who underwent preoperative 16-section MDCT carotid angiography with postoperative microCT and histological evaluation of the CEA specimen [23]. Despite using more modern preoperative CT scanners with 0.5 mm thick reconstructed axial images on their in vivo carotid CTA, there was a significant overlap in HU measurements between fibrous tissue and LRNC. The authors did note that if they restricted the analysis to large LRNC (>5 pixels in diameter), there was a greater concordance between CTA and histology ($\kappa = 0.796$, $P < 0.001$).

In a more recent study of 51 patients with suspected ischemic stroke or transient ischemic attack (TIA) who underwent MDCT carotid angiography and multicontrast carotid plaque MRI within 14 days of the event, a significantly lower HU was detected in plaque containing LRNC or plaque with IPH contained in the LRNC region compared to fibrous plaque [24].

Very recently a new post-processing algorithm using lumen boundary to detect and mitigate blurring and partial volume effects and fit a patient-specific point spread function to the original CTA data has been developed to more accurately measure LRNC and CA [25]. When comparing the preoperative carotid CTA using multiple modern MDCT scanners in 31 consecutive patients scheduled for CEA with postoperative specimen histology, there were a high correlation and low bias between the in vivo software analysis and ex vivo histopathological quantitative measurements of LRNC as well as low reader variability even in the presence of extensive plaque CA (Fig. 5.3).

In summary, there were initial conflicting results when comparing the detection and quantification of LRNC using simple HU measurements on carotid CTA compared with histological evaluation of carotid CEA specimens. As the research and technology have evolved, it now appears that the combination of modern MDCT scanners and a recent post-processing algorithm to mitigate blurring and partial volume effects is now possible to measure carotid plaque LRNC with high correlation and low bias compared with histology.

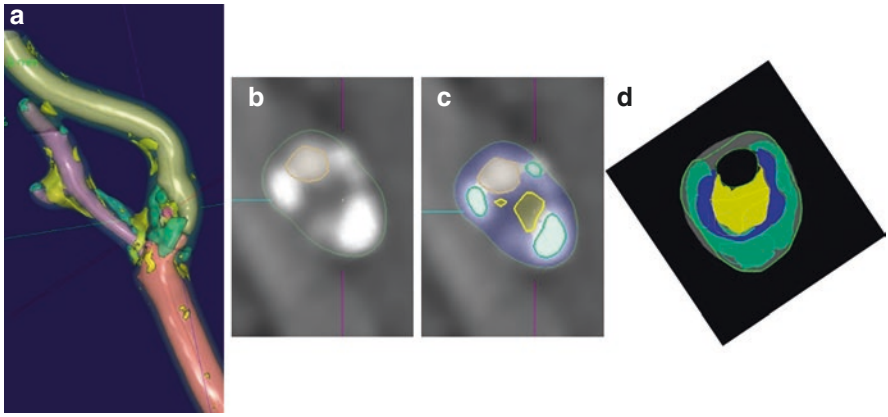

Fig. 5.3 Example of severe stenosis internal carotid artery. (**a**) Three-dimensional segmentation of lumen, vessel wall, and plaque components performed. (**b**) Magnified raw CT angiographic oblique axial image at the level of maximum stenosis shown as green line in part **a**. (**c**) Same level with the segmentation results superimposed (residual lumen outlined by dashed line, yellow outline = LRNC, green outline = calcifications). (**d**) Overlay of regions derived from CT angiography and histologic examination. Histologic sections are shown in solid colors, and results of software analysis are shown in outline. (Yellow = LRNC, green = calcification, blue = fibrosis post-processing using vascuCAP, Elucid Bioimaging Inc., Wenham, MA. ClinicalTrials.gov Identifier: NCT02143102. Images courtesy of Andrew Buckler and Samantha St. Pierre)

Intraplaque Hemorrhage

The literature suggests that accurate detection and quantification of IPH with carotid CTA is even more difficult than LRNC quantification. We will review the research to detect IPH with direct HU measurements as well as indirect detection using general plaque morphology to imply the presence of IPH.

Adjuk et al. analyzed the HU measurements of carotid plaque in the preoperative carotid CTA obtained with a 16-row MDCT scanner in 2 studies of 31 and 50 patients with CEA specimen correlation. They obtained three measurements using a 2 mm diameter region of interest on the 0.7 mm thick axial image in the visually lowest attenuated portion of the plaque and record the lowest of the 3 measurements for comparison with histology. Some of these low attenuation regions were adjacent to CA. Using 33.8 HU as the IPH cutoff value, CTA had 100% sensitivity and 64.7–70.4% specificity to detect IPH.

In a comparison of 167 patients with suspected carotid stenosis who underwent a 4-row or 64-row MDCT carotid angiogram and 1.5T MRA with magnetization-prepared rapid acquisition gradient echo (MPRAGE) sequence using an 8-channel large field-of-view neurovascular coil obtained within 3 weeks, the mean HU for MRI+ IPH was higher (47 HU) compared with MRI- IPH (43 HU). However, significant overlap between distributions of plaque densities limited the value of mean plaque density for prediction of IPH [26].

In the previously described comparison of 8 patients with recent TIA who underwent preoperative 16-section MDCT carotid angiography with postoperative microCT and histological evaluation of the CEA specimen, the authors found the HU measurements of IPH to be higher than fibrous tissue with a cutoff value of 72 HU [23]. As with LRNC and fibrous tissue in the same study, the authors found significant overlap between the HU measurements of IPH and fibrous tissue which limits the value of HU to determine various plaque components. The authors did note that by restricting their analysis to large (>5 pixel) IPH, there was a greater concordance between CTA and histology ($\kappa = 0.712$, $P = 0.102$).

In a more recent publication of 91 patients undergoing preoperative carotid CTA using a 16-row MDCT scanner with 0.6 mm slice thickness, a low average value (18.4 HU) was found for IPH. Using a threshold of 25 HU, IPH presence was detected with a sensitivity of 93.2% and a specificity of 92.7% compared with histopathological evaluation of the CEA specimen [27].

There is an almost equal number of publications demonstrating that IPH has simple HU measurements lower than or higher than fibrous tissue using either histological validation or comparison with MPRAGE. There is no clear way to reconcile these discrepant findings. IPH detection on MDCT carotid angiography using the newly developed post-processing algorithm to mitigate blurring and partial volume effects is an area of current research.

Given the discrepancies in using simple HU to detect IPH, other authors have exploited indirect findings on carotid CTA to detect IPH and/or AHA-LT6 plaques which in part can contain IPH. To date, CTA is not able to reliably identify complicated AHA-TL6 plaques, which are characterized by fibrous cap rupture, attached thrombus, or plaque hemorrhage. Multi-contrast MRI using dedicated carotid plaque surface coils has been shown to accurately identify AHA-LT6 plaques which are closely associated with an increased clinical risk of stroke.

Trelles et al. reported a study of 51 patients with suspected stroke/TIA who underwent multi-contrast carotid MRI with dedicated surface coils and MDCT carotid angiography within 14 days of the event/hospitalization [24]. The maximum soft plaque component thickness proved the best discriminating factor to predict AHA-LT6 by MR imaging, with a receiver operating characteristic area under the curve of 0.89. The optimal sensitivity and specificity for detection of AHA-LT6 by MR imaging was achieved with a soft plaque component thickness threshold of 4.4 mm (sensitivity, 0.65; specificity, 0.94; positive predictive value, 0.75; and negative predictive value, 0.9).

Eisenmenger et al. took a different approach to find an indirect sign of IPH [28]. Because adventitial inflammation is highly associated with IPH and chronic inflammation is associated with calcification, they undertook a retrospective study of 96 patients who underwent a multi-contrast carotid MRI with dedicated surface coils and MDCT carotid angiography within 1 month of each other to determine whether adventitial calcification with internal soft plaque (rim sign) could aid in carotid IPH prediction. A positive rim sign was defined as adventitial calcification (<2-mm thick) with internal soft plaque (≥2-mm thickness). Their final model included the rim sign (prevalence ratio = 11.9, $P < .001$) and

maximum soft plaque thickness (prevalence ratio = 1.2, $P = .06$). This model had excellent intraplaque hemorrhage prediction (area under the curve = 0.94), outperforming the rim sign alone, maximum soft plaque thickness, NASCET stenosis, and ulceration (area under the curve = 0.88, 0.86, 0.77, and 0.63, respectively; $P < .001$).

In summary, there are conflicting results using simple HU to detect IPH. The potential to use the recently described post-processing algorithm to mitigate blurring and reduce partial volume effects to improve IPH detection/quantification is an active area of research. Currently, the best recommendation is to use indirect findings such as the rim sign and maximum thickness of soft tissue plaque to suggest the presence of IPH and/or AHA-LT6 plaque.

Fissured Fibrous Cap

Wintermark et al. developed an automated carotid plaque classification algorithm to identify LRNC and IPH which showed good correlation with histology only when larger LRNC and IPH were considered. They also reported the linear regression between CTA and histology examination was excellent for mean minimal and mean maximal fibrous cap thickness [23]. This technique has not been validated in a separate set of patients. Saba et al. evaluated diffuse plaque enhancement when manually comparing pre-contrast and post-contrast carotid CTA to predict the presence of a fissured fibrous cap [27]. They demonstrated that both plaque neovascularization and fissured fibrous cap were associated with plaque enhancement. Histologic analysis showed that the presence of fissured fibrous cap is associated with a larger contrast plaque enhancement compared with the contrast plaque enhancement of plaques without fissured fibrous cap. The authors noted the increased radiation dose required to calculate the contrast enhancement and hypothesized that future radiation reduction techniques could help make the approach more suitable for clinical use.

CTA Summary

General wisdom says that CT is best to evaluate high-contrast structures (bone, lung, etc.) and MR is best to detect low-contrast soft tissue abnormalities. The extensive literature detailing MR techniques to identify carotid plaque characteristics and the prognostic significance of MR plaque features as well as using MR plaque findings to monitor medical therapy effectiveness supports this general wisdom. Recent research now indicates that CTA can also be used to detect LRNC with high correlation and low bias compared with histology. Even without the use of this new post-processing algorithm, there appears to be value in reviewing the source

axial CTA images to measure the thickness of soft tissue plaque and describe low attenuation regions within the soft tissue plaque to suggest the presence of vulnerable plaque including LRNC. The role of CTA to detect IPH and fibrous cap abnormalities is less clear. Given the ubiquitous use of CTA to evaluate carotid disease, there may be value to include LRNC detection in the routine workup of patients with suspected carotid stenosis. Put another way, do not just report carotid stenosis on CTA neck exams. Despite the new research, there are no randomized controlled trials or even natural history cohort studies to clarify the role of CTA-detected LRNC to predict future ipsilateral stroke/TIA. The role of carotid CTA to evaluate the change in LRNC volume with changes in medical therapy has not been tested, and the impact of multiple CTA exams with its radiation dose needs to be taken into consideration.

Ultrasound Carotid Plaque Imaging

Introduction

Duplex ultrasound is the most widely available noninvasive imaging modality for assessment of carotid plaque. Carotid ultrasound allows for real-time assessment of both plaque morphological characteristics and blood flow. Increasing evidence supports characterization of plaque morphology using ultrasound in risk stratification of patients with both asymptomatic and symptomatic carotid disease, as highlighted in meta-analyses [29, 30]. Established techniques such as B-mode ultrasound as well as newer generation technologies such as contrast-enhanced ultrasound and three-dimensional ultrasound provide extensive information surrounding plaque morphology that may be used for prognostication and interventional consideration.

Techniques

Grayscale ultrasound morphological features of carotid plaques include echogenicity, surface characteristics, and the presence of plaque ulceration. Grayscale ultrasonography can be used to identify non-calcified hypoechoic plaque regions which have been shown to be an independent risk factor for stroke [31]. B-mode ultrasonography allows delineation of vessel wall and is used to assess plaque echogenicity with strong histopathologic correlation [1, 32]. Grayscale carotid plaque echogenicity has been originally stratified into four types by Gray-Weale and colleagues: purely hypoechoic (type I), hypoechoic with small hyperechoic areas (type II), hyperechoic with small hypoechoic areas (type III), and hyperechoic (type IV) [33]. Echolucency is strongly correlated with plaque vulnerability and stroke risk in patients with asymptomatic carotid stenosis; in a 2015 meta-analysis of seven

studies comprising 7557 patients, the relative risk of future ipsilateral stroke with echolucent plaque was 2.31, independent of stenosis degree (95% confidence interval 1.58–3.39, $p < 0.0001$) [29]. A meta-analysis of 23 studies comprising 6706 carotid plaques showed echolucency to occur nearly four times as frequently in symptomatic plaques compared to asymptomatic plaques [30]. In an attempt to standardize images and mitigate inter-observer variability, the median grayscale content of each plaque following normalization of pixel brightness using blood column and adventitia has been used by certain study authors [34]. Others have extended this concept by quantifying the specific pixel intensities of various plaque components on B-mode images, including fibrous tissue, blood, calcium, and lipid and then mapped these to normalized carotid plaque images, termed pixel distribution analysis [35]. This analysis demonstrates symptomatic plaques to have larger quantities of calcium, intraplaque hemorrhage, and lipid, compared to asymptomatic plaques.

B-mode carotid ultrasound is highly specific for identification of plaque surface ulceration though ultrasound-visible ulceration is not always a widespread feature of symptomatic plaques. Additionally, substantial variability exists in the incidence of plaque ulceration as detected on ultrasound [36]. Pulse and color Doppler ultrasound allow for quantification of several flow parameters including peak systolic velocity, end-diastolic velocity, and performance of spectral waveform analysis for assessment of luminal stenosis. While this technique is inexpensive and portable and provides direct information regarding flow, this modality is operator-dependent and is associated with inconsistent inter-observer agreement. Moreover, the correlation of duplex ultrasonography with angiographically determined stenosis is poor [37]. Doppler ultrasound assessment of plaque vulnerability has lower specificity and sensitivity compared to black-blood fat-suppressed MRI sequences; it has been suggested that ultrasound may not be sufficient to identify LRNC vs fibrous plaque for surgical decision-making [38, 39].

Contrast-enhanced ultrasound (CEUS) is a relatively novel technique that utilizes intravenous microbubble contrast agent to assess vessel lumen, intraplaque morphology, and, in particular, neovascularization. Microbubbles are produced from an inert gas and can be contained within a hydrophobic shell for stability [35]. Importantly, microbubble contrast is not nephrotoxic and is associated with minimal side effects. Ultrasound pulses are used to suppress tissue signal, thereby amplifying signal from contrast bubbles. Following injection, microbubbles move into the vasa vasorum and intraplaque microvessels. The vasa vasorum is identified by the presence of echogenic microbubbles in the adventitial layer, while intraplaque vessels are identified by movement of microbubbles from adventitia to plaque core. Thus, plaque and intima-media interface appear hypoechoic, while lumen and wall appear enhanced. Both expanded vasa vasorum and intraplaque neovascularization are associated with advanced lesions.

Plaque enhancement with microbubble contrast is markedly higher in symptomatic plaques and associated with increased cardiovascular events, though not always histologically corroborative with plaque morphology [40–42]. Uniquely, CEUS allows for visualization of plaque heterogeneity both spatially and temporally with-

out exposure to ionizing radiation (Johri et al. 2017). Intraplaque vessel size as determined by CEUS has also recently been significantly associated with carotid plaque histology (Amamoto Cerebovasc Dis 2018). Persisting plaque enhancement following contrast administration is suggested to reflect increased intraplaque inflammatory cells, which phagocytize microbubbles and adhere to adjacent endothelium, termed "late-phase enhancement" [43]. Though an informative technique, CEUS is similarly operator-dependent and contraindicated in several conditions, including acute heart failure, unstable angina, and right-to-left cardiac shunts [44].

Three-dimensional (3-D) ultrasound is another novel technique that has garnered interest in recent years. Though two-dimensional B-mode images are readily obtainable, the single slice provides limited information. Importantly, 3-D imaging mitigates the inherent operator dependence of two-dimensional ultrasonography. Segmented image acquisition is performed longitudinally along the plaque, bounded by vessel wall; these images are then stacked and collated to produce volume -rendered reconstructions. In small preliminary studies, 3-D ultrasound has shown excellent specificity for the evaluation of stenosis and for measurement of plaque volume [45, 46]. Volumetric quantification allows plaque components to be identified based on tissue volumes, including hemorrhage, lipid, and calcium. Plaque composition is furthermore readily characterized using 3-D protocols, and plaque volume changes as small as 5% are detectable [35, 47]. However, 3-D ultrasound is more time-consuming than traditional two-dimensional ultrasound. Inter- and intra-observer reliabilities are substantially lower than compared to conventional ultrasound.

Ultrasound elastography is another technique that has been used in other organs, namely, breast and thyroid, and has recently been applied to carotid plaque imaging. This modality takes advantage of radial and longitudinal displacement of the plaque in response to artery pulsation and enables plaque motion to be tracked using registration and visualized displacement vectors [35]. Elastography analysis enables determination of strain and translation in both axial and longitudinal axes. Carotid plaque elasticity has been corroborated with intraplaque neovascularization as seen on CEUS [48]. Furthermore, axial strain and translation have been reported to be higher in vulnerable, neovascularized plaques with corollary MRI [49, 50]. These results suggest a potential role for quantitative analysis of plaque morphology through measurement of displacement parameters.

Poor signal-to-noise and moderate spatial resolutions make intraplaque hemorrhage difficult to distinguish from lipid-rich necrotic core on ultrasound. On B-mode imaging, the necrotic core can appear hypoechoic in appearance, also known as a juxtaluminal black area. Histologically, this region correlates with a lipid core that is adjacent to the vessel lumen. A juxtaluminal black area of 8 mm^2 has been shown to be highly prevalent in symptomatic plaques and independently associated with neurological symptoms [51]. Furthermore, in the analysis of 1121 patients with asymptomatic carotid stenosis, the juxtaluminal black area was linearly associated with future stroke rate, with 0.4% risk in patients with area less than 4 mm^2 and 5% risk in patients with area greater than 10 mm [2, 52]. In this study, the juxtaluminal black area was defined as an area of pixels with grayscale value less than 25 without an evident echogenic cap (grayscale greater than 25).

Ultrasound Summary

Ultrasound has remained the workhorse imaging modality for carotid plaque imaging, though the technique is limited by operator dependence, non-optimal spatial and contrast resolution, and inter-observer variability. Unlike other modalities, however, ultrasonography is inexpensive, widely available and does not pose risk of radiation exposure or contrast nephrotoxicity. Importantly, Doppler ultrasound remains a key modality for real-time assessment of flow and carotid stenosis. Newer generation improvements to ultrasonography include administration of microbubble contrast and three-dimensional image acquisition. These techniques allow for improved assessment of plaque vulnerability via intraplaque neovascularization with markedly higher inter-observer reliability. The utility of carotid ultrasonography in selecting patients for carotid endarterectomy based on degree of stenosis and plaque characteristics, however, remains to be determined.

Disclaimer The views expressed in this chapter are those of the author and do not reflect the official policy of the Department of Army/Navy/Air Force, Department of Defense, or US Government.

The identification of specific products or scientific instrumentation does not constitute endorsement or implied endorsement on the part of the author, DoD, or any component agency.

References

1. Brinjikji W, Lehman VT, Huston J 3rd, et al. The association between carotid intraplaque hemorrhage and outcomes of carotid stenting: a systematic review and meta-analysis. J Neurointerv Surg. 2017;9(9):837–42.
2. Kerwin WS, O'Brien KD, Ferguson MS, Polissar N, Hatsukami TS, Yuan C. Inflammation in carotid atherosclerotic plaque: a dynamic contrast-enhanced MR imaging study. Radiology. 2006;241(2):459–68.
3. Millon A, Mathevet JL, Boussel L, et al. High-resolution magnetic resonance imaging of carotid atherosclerosis identifies vulnerable carotid plaques. J Vasc Surg. 2013;57(4):1046–1051.e1042.
4. den Hartog AG, Bovens SM, Koning W, et al. Current status of clinical magnetic resonance imaging for plaque characterisation in patients with carotid artery stenosis. Eur J Vasc Endovasc Surg. 2013;45(1):7–21.
5. Chan JM, Monaco C, Wylezinska-Arridge M, Tremoleda JL, Gibbs RG. Imaging of the vulnerable carotid plaque: biological targeting of inflammation in atherosclerosis using iron oxide particles and MRI. Eur J Vasc Endovasc Surg. 2014;47(5):462–9.
6. Chu B, Kampschulte A, Ferguson MS, et al. Hemorrhage in the atherosclerotic carotid plaque: a high-resolution MRI study. Stroke. 2004;35(5):1079–84.
7. Moody AR, Murphy RE, Morgan PS, et al. Characterization of complicated carotid plaque with magnetic resonance direct thrombus imaging in patients with cerebral ischemia. Circulation. 2003;107(24):3047–52.
8. Moody AR. Magnetic resonance direct thrombus imaging. J Thromb Haemost. 2003;1(7):1403–9.
9. Singh N, Moody AR, Roifman I, Bluemke DA, Zavodni AE. Advanced MRI for carotid plaque imaging. Int J Cardiovasc Imaging. 2016;32(1):83–9.

10. Kampschulte A, Ferguson MS, Kerwin WS, et al. Differentiation of intraplaque versus juxtaluminal hemorrhage/thrombus in advanced human carotid atherosclerotic lesions by in vivo magnetic resonance imaging. Circulation. 2004;110(20):3239–44.
11. Yim YJ, Choe YH, Ko Y, et al. High signal intensity halo around the carotid artery on maximum intensity projection images of time-of-flight MR angiography: a new sign for intraplaque hemorrhage. J Magn Reson Imaging. 2008;27(6):1341–6.
12. Chu B, Hatsukami TS, Polissar NL, et al. Determination of carotid artery atherosclerotic lesion type and distribution in hypercholesterolemic patients with moderate carotid stenosis using noninvasive magnetic resonance imaging. Stroke. 2004;35(11):2444–8.
13. Singh N, Moody AR, Gladstone DJ, et al. Moderate carotid artery stenosis: MR imaging-depicted intraplaque hemorrhage predicts risk of cerebrovascular ischemic events in asymptomatic men. Radiology. 2009;252(2):502–8.
14. Saam T, Hetterich H, Hoffmann V, et al. Meta-analysis and systematic review of the predictive value of carotid plaque hemorrhage on cerebrovascular events by magnetic resonance imaging. J Am Coll Cardiol. 2013;62(12):1081–91.
15. Cappendijk VC, Heeneman S, Kessels AG, et al. Comparison of single-sequence T1w TFE MRI with multisequence MRI for the quantification of lipid-rich necrotic core in atherosclerotic plaque. J Magn Reson Imaging. 2008;27(6):1347–55.
16. Yuan C, Kerwin WS, Ferguson MS, et al. Contrast-enhanced high resolution MRI for atherosclerotic carotid artery tissue characterization. J Magn Reson Imaging. 2002;15(1):62–7.
17. Cai J, Hatsukami TS, Ferguson MS, et al. In vivo quantitative measurement of intact fibrous cap and lipid-rich necrotic core size in atherosclerotic carotid plaque: comparison of high-resolution, contrast-enhanced magnetic resonance imaging and histology. Circulation. 2005;112(22):3437–44.
18. Serfaty JM, Chaabane L, Tabib A, Chevallier JM, Briguet A, Douek PC. Atherosclerotic plaques: classification and characterization with T2-weighted high-spatial-resolution MR imaging-- an in vitro study. Radiology. 2001;219(2):403–10.
19. Qiao Y, Etesami M, Astor BC, Zeiler SR, Trout HH, Wasserman BA. Carotid plaque neovascularization and hemorrhage detected by MR imaging are associated with recent cerebrovascular ischemic events. AJNR Am J Neuroradiol. 2012;33(4):755–60.
20. Gupta A, Baradaran H, Schweitzer AD, et al. Carotid plaque MRI and stroke risk: a systematic review and meta-analysis. Stroke. 2013;44(11):3071–7.
21. Walker LJ, Ismail A, McMeekin W, Lambert D, Mendelow AD, Birchall D. Computed tomography angiography for the evaluation of carotid atherosclerotic plaque: correlation with histopathology of endarterectomy specimens. Stroke. 2002;33(4):977–81.
22. de Weert TT, Ouhlous M, Meijering E, et al. In vivo characterization and quantification of atherosclerotic carotid plaque components with multidetector computed tomography and histopathological correlation. Arterioscler Thromb Vasc Biol. 2006;26(10):2366–72.
23. Wintermark M, Jawadi SS, Rapp JH, et al. High-resolution CT imaging of carotid artery atherosclerotic plaques. AJNR Am J Neuroradiol. 2008;29(5):875–82.
24. Trelles M, Eberhardt KM, Buchholz M, et al. CTA for screening of complicated atherosclerotic carotid plaque--American Heart Association type VI lesions as defined by MRI. AJNR Am J Neuroradiol. 2013;34(12):2331–7.
25. Sheahan M, Ma X, Paik D, et al. Atherosclerotic plaque tissue: noninvasive quantitative assessment of characteristics with software-aided measurements from conventional CT angiography. Radiology. 2018;286(2):622–31.
26. JM UK-I, Fox AJ, Aviv RI, et al. Characterization of carotid plaque hemorrhage: a CT angiography and MR intraplaque hemorrhage study. Stroke. 2010;41(8):1623–9.
27. Saba L, Francone M, Bassareo PP, et al. CT attenuation analysis of carotid intraplaque hemorrhage. AJNR Am J Neuroradiol. 2018;39(1):131–7.
28. Eisenmenger LB, Aldred BW, Kim SE, et al. Prediction of carotid intraplaque hemorrhage using adventitial calcification and plaque thickness on CTA. AJNR Am J Neuroradiol. 2016;37(8):1496–503.

29. Gupta A, Kesavabhotla K, Baradaran H, et al. Plaque echolucency and stroke risk in asymptomatic carotid stenosis: a systematic review and meta-analysis. Stroke. 2015;46(1):91–7.
30. Brinjikji W, Rabinstein AA, Lanzino G, et al. Ultrasound characteristics of symptomatic carotid plaques: a systematic review and meta-analysis. Cerebrovasc Dis. 2015;40(3–4):165–74.
31. Polak JF, Shemanski L, O'Leary DH, et al. Hypoechoic plaque at US of the carotid artery: an independent risk factor for incident stroke in adults aged 65 years or older. Cardiovascular Health Study. Radiology. 1998;208(3):649–54.
32. Reiter M, Horvat R, Puchner S, et al. Plaque imaging of the internal carotid artery - correlation of B-flow imaging with histopathology. AJNR Am J Neuroradiol. 2007;28(1):122–6.
33. Gray-Weale AC, Graham JC, Burnett JR, Byrne K, Lusby RJ. Carotid artery atheroma: comparison of preoperative B-mode ultrasound appearance with carotid endarterectomy specimen pathology. J Cardiovasc Surg. 1988;29(6):676–81.
34. el-Barghouty N, Nicolaides A, Bahal V, Geroulakos G, Androulakis A. The identification of the high risk carotid plaque. Eur J Vasc Endovasc Surg. 1996;11(4):470–8.
35. Cires-Drouet RS, Mozafarian M, Ali A, Sikdar S, Lal BK. Imaging of high-risk carotid plaques: ultrasound. Semin Vasc Surg. 2017;30(1):44–53.
36. Nakamura T, Tsutsumi Y, Shimizu Y, Uchiyama S. Ulcerated carotid plaques with ultrasonic echolucency are causatively associated with thromboembolic cerebrovascular events. J Stroke Cerebrovasc Dis. 2013;22(2):93–9.
37. Beach KW, Leotta DF, Zierler RE. Carotid Doppler velocity measurements and anatomic stenosis: correlation is futile. Vasc Endovasc Surg. 2012;46(6):466–74.
38. Arai D, Yamaguchi S, Murakami M, et al. Characteristics of carotid plaque findings on ultrasonography and black blood magnetic resonance imaging in comparison with pathological findings. Acta Neurochir Suppl. 2011;112:15–9.
39. Watanabe Y, Nagayama M, Suga T, et al. Characterization of atherosclerotic plaque of carotid arteries with histopathological correlation: vascular wall MR imaging vs. color Doppler ultrasonography (US). J Magn Reson Imaging. 2008;28(2):478–85.
40. Vavuranakis M, Sigala F, Vrachatis DA, et al. Quantitative analysis of carotid plaque vasa vasorum by CEUS and correlation with histology after endarterectomy. VASA Zeitschrift fur Gefasskrankheiten. 2013;42(3):184–95.
41. Xiong L, Deng YB, Zhu Y, Liu YN, Bi XJ. Correlation of carotid plaque neovascularization detected by using contrast-enhanced US with clinical symptoms. Radiology. 2009;251(2):583–9.
42. Staub D, Patel MB, Tibrewala A, et al. Vasa vasorum and plaque neovascularization on contrast-enhanced carotid ultrasound imaging correlates with cardiovascular disease and past cardiovascular events. Stroke. 2010;41(1):41–7.
43. Owen DR, Shalhoub J, Miller S, et al. Inflammation within carotid atherosclerotic plaque: assessment with late-phase contrast-enhanced US. Radiology. 2010;255(2):638–44.
44. Ten Kate GL, van den Oord SC, Sijbrands EJ, et al. Current status and future developments of contrast-enhanced ultrasound of carotid atherosclerosis. J Vasc Surg. 2013;57(2):539–46.
45. Landry A, Spence JD, Fenster A. Measurement of carotid plaque volume by 3-dimensional ultrasound. Stroke. 2004;35(4):864–9.
46. Bucek RA, Reiter M, Dirisamer A, et al. Three-dimensional color Doppler sonography in carotid artery stenosis. AJNR Am J Neuroradiol. 2003;24(7):1294–9.
47. Hossain MM, AlMuhanna K, Zhao L, Lal BK, Sikdar S. Semiautomatic segmentation of atherosclerotic carotid artery wall volume using 3D ultrasound imaging. Med Phys. 2015;42(4):2029–43.
48. Zhang Q, Li C, Zhou M, et al. Quantification of carotid plaque elasticity and intraplaque neovascularization using contrast-enhanced ultrasound and image registration-based elastography. Ultrasonics. 2015;62:253–62.

49. Huang C, Pan X, He Q, et al. Ultrasound-based carotid elastography for detection of vulnerable atherosclerotic plaques validated by magnetic resonance imaging. Ultrasound Med Biol. 2016;42(2):365–77.
50. Roy Cardinal MH, Heusinkveld MHG, Qin Z, et al. Carotid artery plaque vulnerability assessment using noninvasive ultrasound elastography: validation with MRI. AJR Am J Roentgenol. 2017;209(1):142–51.
51. Griffin MB, Kyriacou E, Pattichis C, et al. Juxtaluminal hypoechoic area in ultrasonic images of carotid plaques and hemispheric symptoms. J Vasc Surg. 2010;52(1):69–76.
52. Kakkos SK, Griffin MB, Nicolaides AN, et al. The size of juxtaluminal hypoechoic area in ultrasound images of asymptomatic carotid plaques predicts the occurrence of stroke. J Vasc Surg. 2013;57(3):609–618.e601; discussion 617-608.